ELSEVIER

Journal of Magnetism and Magnetic Materials 237 (2001) 47–54

Journal of magnetism and magnetic materials

www.elsevier.com/locate/jmmm

Coulomb correlation and magnetic ordering in double-layered manganites: $LaSr_2Mn_2O_7$

Julia E. Medvedeva[a,b], Vladimir I. Anisimov[b], Michael A. Korotin[b], Oleg N. Mryasov[a], Arthur J. Freeman[a,*]

[a] *Science and Technical Center for Superconduction, Department of Physics and Astronomy, Northwestern University, 2145 NO, Sheridan Road, Evanston, IL 60208-3112, USA*

[b] *Institute of Metal Physics, Yekaterinburg 620219, Russia*

Received 25 April 2001; received in revised form 3 August 2001

Abstract

A detailed study of the electronic structure and magnetic configurations of the 50% hole-doped double-layered manganite $LaSr_2Mn_2O_7$ is presented. We demonstrate that the on-site Coulomb correlation (U) of Mn d electrons (i) significantly modifies the electronic structure, magnetic ordering (from FM to AFM), and interlayer exchange interactions, and (ii) promotes strong anisotropy in electrical transport, reducing the effective hopping parameter along the c-axis for electrically active e_g electrons. This finding is consistent with observations of anisotropic transport—a property which sets this manganite apart from conventional 3D systems. A half-metallic band structure is predicted with both the LSDA and LSDA + U methods. The experimentally observed A-type AFM ordering in $LaSr_2Mn_2O_7$ is found to be energetically more favorable with $U \geqslant 7$ eV. A simple interpretation of interlayer exchange coupling is given within double and super-exchange mechanisms based on the dependencies on U of the effective exchange parameters and e_g state sub-band widths.

Keywords: Double-layered manganite; Anisotropy in electrical transport; Half-metallic

1. Introduction

The double-layered CMR manganite materials, $La_{2-2x}Sr_{1+2x}Mn_2O_7$ [1], demonstrate magnetic behavior that is distinct from the perovskite manganites, $La_{1-x}Sr_xMnO_3$, including: (i) strong anisotropy of electrical (magneto-) transport [1–4]; (ii) nearly two-dimensional (2D) character of its magnetism and strong AFM magnetic correlations above T_c [5]; and (iii) anomalous magnetoelastic properties [4].

Most experimental reports on the layered manganites have concentrated on the $La_{2-2x}Sr_{1+2x}Mn_2O_7$ compounds with $x \approx 0.4$, which are metallic and demonstrate strong magnetoresistive effects. Stochiometric $LaSr_2Mn_2O_7$ ($x = 0.5$) exhibits interesting spin, charge and orbital ordering, and its resistivity is of the order of $10^{\circ}\,\Omega$ cm with a rather flat temperature dependence [6]. This can be compared with the situation in perovskite manganites where undoped $LaMnO_3$ is an antiferromagnetic insulator with

*Corresponding author. Tel.: +1-847-491-3343; fax: +1-847-491-5082.

E-mail address: art@freeman.phys.nwu.edu (A.J. Freeman).

0304-8853/01/$ - see front matter
PII: S0304-8853(01)00487-5

strong orbital ordering and $La_{1-x}Sr_xMnO_3$ with $x \approx 0.4$ is a metal with strong magnetoresistive effects [7].

In comparison with the pseudocubic perovskites with 3D networks of MnO_6 octahedra (i.e. $(La,Sr)MnO_3$), these layered structures $(La,Sr)_3Mn_2O_7$ have a reduced exchange coupling between the Mn ions along the *c* direction. Indeed, the pseudocubic perovskites show ferromagnetism and metallic conductivity over a wide range of hole doping, suggesting that the double-exchange mechanism is dominant among itinerant e_g electrons. In the double-layered case, with the 2D Mn–O network, consisting of two perovskite blocks separated by an intervening insulating layer of (La,Sr)O ions along the *c*-axis, the balance between antiferromagnetism and ferromagnetism is very sensitive to e_g band filling [8]. Bilayer $La_{2-2x}Sr_{1+2x}Mn_2O_7$ demonstrates ferromagnetism in a doping range $x < 0.39$, a canted antiferromagnetic structure for a hole concentration $0.39 < x < 0.48$, and layered antiferromagnetic states for $x > 0.48$ [9,10].

From experimental data [6,8,10–13], it is known that the ground state spin structure of $LaSr_2Mn_2O_7$ phase is A-type-layered antiferromagnet (AFM), where the magnetic moments lie in the *ab* plane and couple ferromagnetically within the single MnO_2 layer, but show AFM order between the respective MnO_2 layers within the bilayer unit. The interlayer coupling in the bilayer stack is ferromagnetic.

One of the most striking properties of the bilayered $LaSr_2Mn_2O_7$ is the competition between the (charge-disordered) A-type AFM spin ordering with a Neél temperature $T_N \approx 170\,K$ and the CE-type [14] charge/orbital ordering which exists between T_N and $T_{CO} = 210\,K$ [13]. With decreasing temperature, the development of the charge/orbital ordering phase is disrupted by the onset of the A-type AFM ordering at T_N—which may be qualitatively explained by the onset of ferromagnetic order in each *ab* plane.

An important issue in the theory of CMR oxides is the role of Coulomb correlation. An accurate treatment of correlation may significantly affect the balance between ferromagnetic and antiferromagnetic interactions and hence the magnetic ground state. LDA band structure calculations for CMR perovskites demonstrated the possibility of LDA theory predicting the correct magnetic ground state [15]. For the double-layered perovskites, an investigation of the reliability of this theory has not yet been performed. In their report on the electronic structure calculations of $LaSr_2Mn_2O_7$ within the general gradient approximation (GGA) [16], Boer and de Groot suggested to take into account some additional correlation corrections to obtain a truly half-metallic electronic structure in the layered manganites. There is one report of an LDA + U calculation [17] performed for the doping level of 0.4 holes per Mn site ($La_{1.2}Sr_{1.8}Mn_2O_7$), but details of their calculation have not been presented and the important question of how correlations affect the magnetic ground state has not been investigated.

The purpose of our work is to study the electronic structure which governs the microscopic origin of the magnetic phenomena in the bilayered manganite, and to determine its dependence on Coulomb correlations and its relation with magnetic properties. We consider the difference in the total energies, exchange interaction parameters, the population of Mn-d and O-p states near the Fermi level and d sub-bandwidths for ferromagnetic (FM) and A-type antiferromagnetic (AFM) configurations as a function of the Coulomb correlation parameter *U* and give a simple interpretation of exchange coupling between Mn layers in $LaSr_2Mn_2O_7$ within the double exchange model. In contrast to the case of $LaMnO_3$, we find that the inclusion of *U* in $LaSr_2Mn_2O_7$ results in important differences in the e_g-band characteristics that are responsible for the observed FM instability and for strong anisotropy in the electrical transport.

2. Methodology

The LSDA and LSDA + U calculations were realized in the frame work of the linear-muffin-tin-orbital method in the atomic sphere approximation (LMTO-ASA) [18]. We used the von Barth et al. form [19] for exchange-correlation potential.

The crystal parameters were taken from Ref. [12]. The atomic sphere radii were: R(La(Sr)) = 3.4 a.u., R(Mn) = 2.8 a.u., and R(O) = 2.2 a.u. From the constrained LSDA supercell calculations [20,21], we obtained values of the Coulomb and exchange parameters to be $U = 7.2$ eV and $J = 0.78$ eV. These values are typical for the transition-metal oxides [22–25].

3. Results and discussion

3.1. Electronic structure

As a first step, we calculated the electronic structure of FM (all atoms in every layer and between layers are ordered ferromagnetically) and A-type AFM (ferromagnetic layers stacked antiferromagnetically) $LaSr_2Mn_2O_7$ by the standard LSDA method ($U = 0$). The total and projected densities of states (DOS) for these cases are shown in Fig. 1. For the majority-spin channel (solid line), Mn 3d states form the bands between 2.2 eV below E_F and 2.5 eV above E_F. As seen from the figure, the e_g ($x^2 - y^2$ and $3z^2 - r^2$) bands are partially filled, cross E_F, and are rather broad compared to the t_{2g} (xy and degenerate xz, yz) bands which are about 1.2 eV wide and lie 1 eV below E_F. The exchange interaction splits the Mn 3d states such that the t_{2g} and e_g minority-spin bands are located 2.6 eV higher in energy than the majority-spin states. We obtained a band gap of 2.5 eV in the minority-spin d bands and a band structure that is in a very good agreement with that obtained by the full-potential LMTO method [26] (but their band gap within the minority-spin channel is about 1.7–1.9 eV). Our results for the ferromagnetic state with $U = 0$ differ from the results of Dessau et al. [17] where a U of 2 eV was used to obtain a gap at E_F in the minority-spin bands for $La_{1.2}Sr_{1.8}Mn_2O_7$. It should be noted that the Fermi level in our calculations was found to lie at the bottom of the t_{2g} minority conduction band (as in the FLMTO calculation [26]), so the electronic structure just misses to being a half-metallic one.

In order to investigate the role of on-site Coulomb correlation, we calculated the electronic structures of $LaSr_2Mn_2O_7$ for both FM and A-type AFM orderings using a number of values of U, namely 2, 4, 6, 7.2, 8, 9 and 10 eV. The total and projected DOSs of the FM and AFM cases with $U = 7.2$ eV are shown in Fig. 2. Only majority e_g states make a significant contribution to the DOS at E_F. For $U = 0$, one can expect 3D conduction in both spin channels (Fig. 1), while for $U > 0$ we obtain a half-metallic state—electron conduction is possible only within majority spin sublattice. We want to emphasize here analogues in the main band characteristics near E_F in the calculated electronic spectra of double-layered and doped perovskite manganites [27]. And since doped perovskite manganites are found to be half-metallic [28,29], this may also be the case for the double-layered manganite.

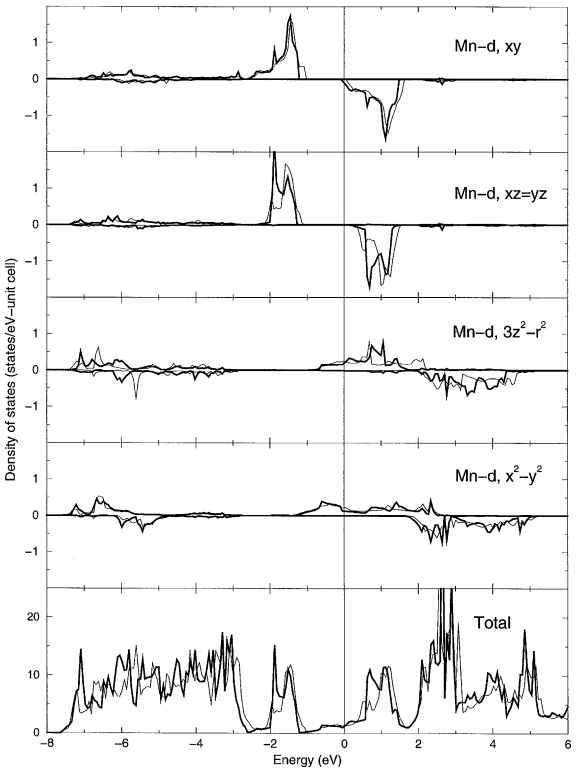

Fig. 1. Calculated LSDA total and projected densities of states (in states/eV-unit cell) of the ferromagnetic (thin line) and antiferromagnetic (thick line) phases. The Fermi level is located at 0 eV.

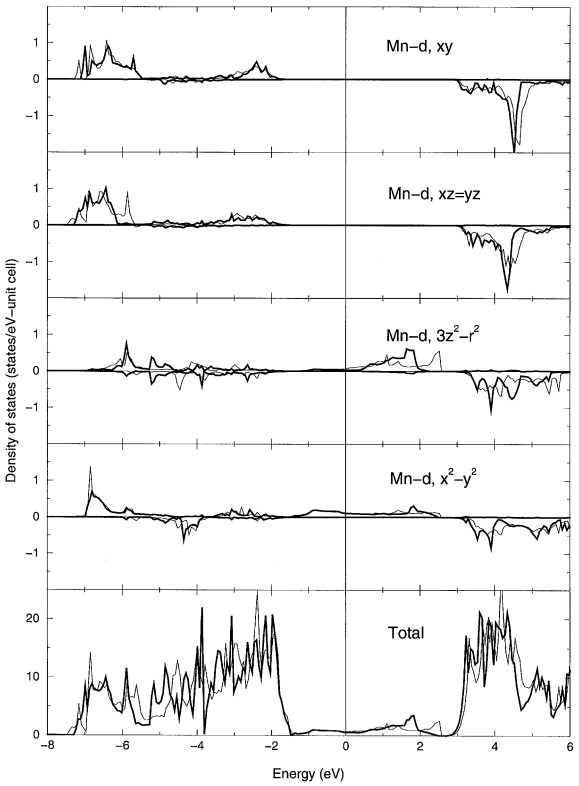

Fig. 2. The total and projected densities of states (in states/eV-unit cell) of the ferromagnetic (thin line) and antiferromagnetic (rich line) phases from the LSDA + U calculation, $U = 7.2$ eV. The Fermi level is located at 0 eV.

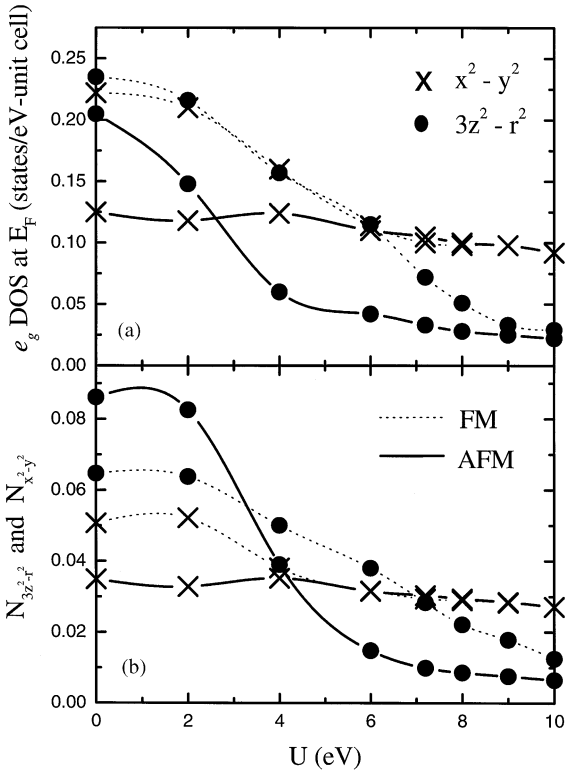

Fig. 3. Contribution of $3z^2 - r^2$ (circles) and $x^2 - y^2$ (crosses) states to (a) the density of states at E_F and (b) the number of states (NOS) integrated in a small energy window of 0.3 eV just above E_F as a function of Coulomb U. Solid and dashed lines correspond to AFM and FM cases, respectivly.

3.2. Anisotropy in electrical transport

To investigate the variation (behavior) of the electrically active states as a function of on-site Coulomb correlation, we plot in Fig. 3 the dependence on U of the $3z^2 - r^2$ and $x^2 - y^2$ states contribution to the DOS at E_F (Fig. 3(a)) and to the number of states integrated in a small energy window of 0.3 eV just above E_F (denoted as $N_{3z^2-r^2}$ and $N_{x^2-y^2}$ in Fig. 3(b)). The difference between FM and AFM phases for a particular U value is clearly seen from Fig. 3(a). For the FM phase (dotted lines), both contributions of the $3z^2 - r^2$ (circles) and $x^2 - y^2$ (crosses) states decrease with U in almost the same way, and only large U values ($U > 7$ eV) result in a splitting of the e_g states. The most significant changes occur for AFM spin alignment (solid lines). The e_g states are already split in the LSDA calculation ($U = 0$) and the difference between the electron population of $3z^2 - r^2$ and $x^2 - y^2$ orbitals is clearly seen (Fig. 3(a)). Further, while the contribution of the $x^2 - y^2$ state to the DOS at E_F does not change with an increase of U, the $3z^2 - r^2$ contribution, which is almost two times bigger than that of $x^2 - y^2$ for $U = 0$, drastically decreases with U, taking its minimum for $U > 7$ eV.

As can be seen from Fig. 3(b), the situation does not change qualitatively in the energy window just above E_F, encouraging us to draw the following conclusions: For small U values we have 3D conduction, while for $U > 6$ the electron conduction (hopping) along the c-axis becomes very

small. Thus, on-site correlation treated within LSDA + U promotes 2D type (in-plane) electronic behavior in the system. We need to add here that the significant difference between $3z^2 - r^2$ and $x^2 - y^2$ states (due to an decrease of the bandwidth as well as a shift to higher energy of the $3z^2 - r^2$ state with increase of U) is an essential feature of $LaSr_2Mn_2O_7$. It sets the double-layered manganite apart from perovskite manganites (i.e. (La,Sr) MnO_3) in which the main energy characteristics such as widths and centers of both e_g bands are very close.

The anisotropy in the population of the two e_g states established above can be illustrated more clearly in the plot of the angular distribution of the electron density in the 0.3 eV energy window above E_F for $U = 0$ and for the calculated value, $U = 7$ eV (cf. Fig. 4). A comparison of the lowest spin configurations (FM for $U = 0$ (Fig. 4(a)) and AFM for $U = 7$ eV (Fig. 4(d)) as obtained from

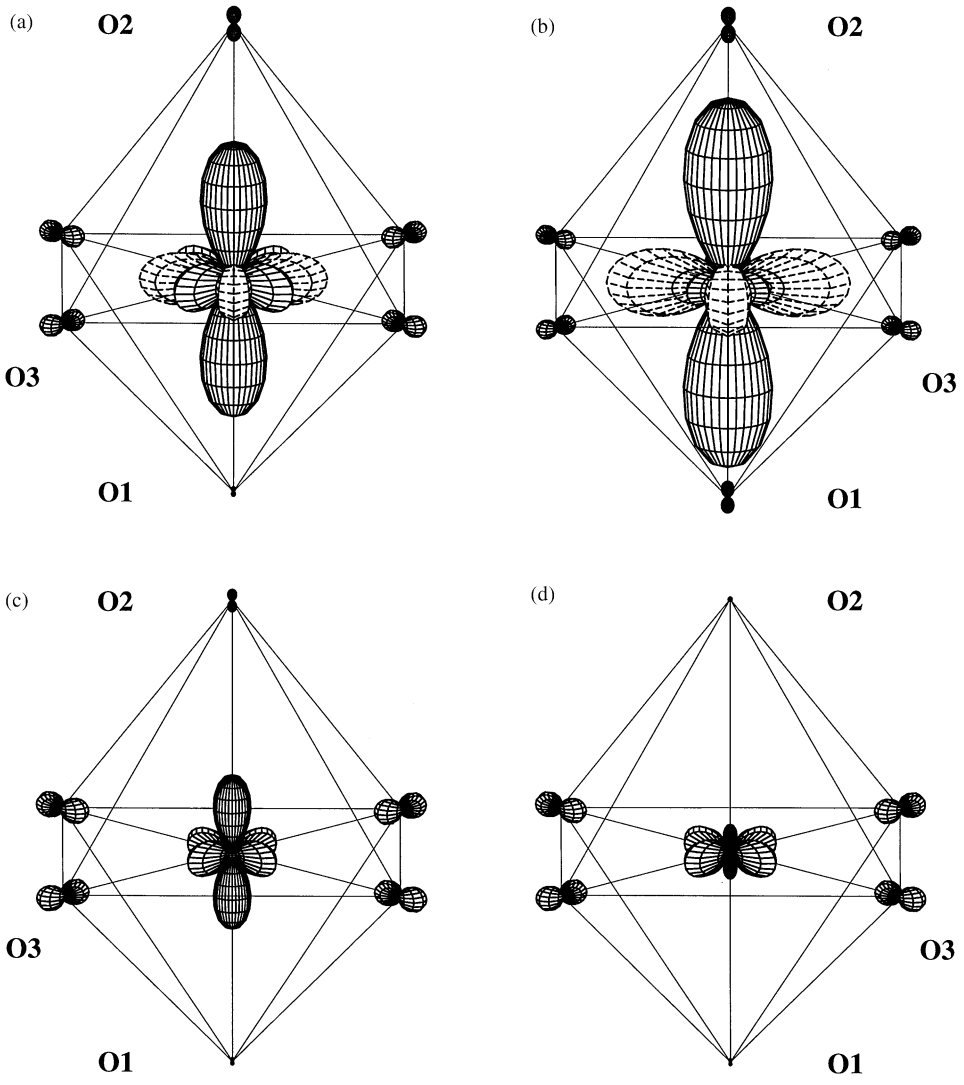

Fig. 4. The calculated angular electron density distribution for the energy window of 0.3 eV width just above E_F for (a) FM, $U = 0$; (b) A-type AFM, $U = 0$; (c) FM, $U = 7.2$ eV and (d) A-type AFM, $U = 7.2$ eV. Only one MnO_6 octahedron which belongs to the upper layer of the bilayer is shown. Solid line is for majority spin and dashed line is for minority spin.

total energy differences) shows that both on-site correlation and change in spin ordering significantly decrease the number of electrons that contribute to electrical transport along the c-axis. This is contrary to the in-plane state which remain less sensitive to the spin alignment change and influence of U. (Note, however, that only on-site correlation supresses the minority $t_{2g}(xy)$ state contribution to the electron density above E_F, resulting in a half-metallic state, as mentioned above.)

The decisive role of the on-site Coulomb correlation in lowering the dimensionality of the conduction band is clearly seen from a comparison of two AFM cases with $U = 0$ and 7 eV (Fig. 4(b) and (d)): for $U = 7$ eV, only the $x^2 - y^2$ orbital has some contribution just above E_F and hopping along the c-axis is negligible (the $3z^2 - r^2$ state is responsible for it). This is consistent with the point that the main issue for realizing the layered AFM state is the strong anisotropy in the population of the 2D $d_{x^2-y^2}$ state and the one-dimensional (1D) $d_{3z^2-r^2}$ state. For the FM state, the orbital configurations have more electron population freedom, because three crystallographic axes are equivalent. Qualitatively this situation does not change as U increases. According to the qualitative picture of the simple double exchange model, an electrically active electron has a finite hopping probability (t) between ferromagnetically ordered Mn ions, but this hopping vanishes in the case of antiferromagnetic spin alignment due to strong Hund coupling ($t \ll J$). Fig. 4(b) clearly shows the failure of the LSDA scheme. Thus, taking into account on-site Coulomb correlation gives us the correct picture of 2D-like charge transport in the layered manganite: the increase of U suppresses the c-axis transport, keeping electron conduction in the ab plane. However, it should be noted that the transition from FM to AFM ordering (Fig. 4(c) and (d)) also contributes to this tendency, but to a lesser degree than on-site correlation—as can be seen from a comparison of Fig. 4(a) and (d).

3.3. Magnetic ordering

To investigate how the magnetic interaction and ground state depend on U, we calculated total energy differences for $U = 0$, 2, 4, 6, 7.2, 8, 9 and 10 eV. The results are shown in Fig. 5(a), where the total energy of the FM spin ordering for each value of U is taken to be zero. Although the difference of the two calculated spin alignments is $\leqslant 0.1$ eV for all cases (and so we have almost degenerate magnetic states), for $U = 0$, 2 and 4 eV the FM ordering is preferred, while for $U = 6$, 7.2, 8, 9 and 10 eV the AFM phase has lower energy. Thus, the on-site Mn-d electron Coulomb correlations modify the magnetic ordering from FM to A-type AFM—as experimentally observed. Note, that the total energy difference between FM and AFM states does not change for $U \geqslant 8$ eV. To determine the character of the exchange coupling in the layered manganite and to understand why the experimentally observed A-type AFM spin ordering is simulated

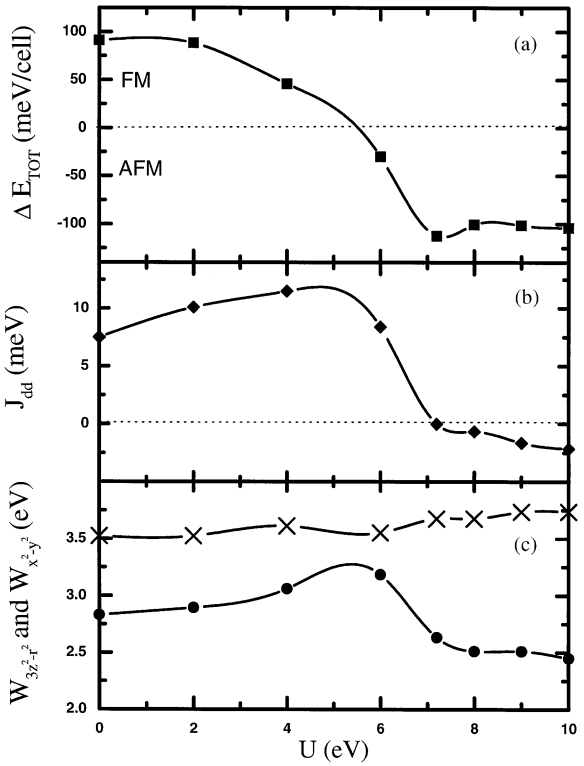

Fig. 5. The influence of U on (a) the total energy difference between FM and A-type AFM phases; (b) the calculated interlayer exchange interaction parameters for FM phase; (c) the width of the $3z^2 - r^2$ (circles) and $x^2 - y^2$ (crosses) bands for FM phase.

only with $U > 7$ eV, we also calculated the effective exchange interaction parameters (for computational details see Ref. [30]). In Fig. 5(b), the values of the d–d effective exchange parameters, J_{dd}, between nearest Mn neighbors which belong to the different layers of one bilayer are shown as a function of U. They are seen to follow the behavior of the total energy differences shown in Fig. 5(a).

Usually, the exchange coupling is described within the superexchange (SEX) and double exchange (DEX) models and corresponding solutions of the simple Hamiltonian problem with the following parameters: hopping between Mn ions (t), J (DEX model); and t, U (SEX model). To provide interpretation to this model, we plot the e_g-sub-bandwidths of the FM phase for a number of U values in Fig. 5(c) (denoted as $W_{3z^2-r^2}$ and $W_{x^2-y^2}$ below). As can be seen, the $x^2 - y^2$ bandwidth almost does not change its value with U, and the main differences in the electronic spectra due to an increase of U are connected with the $3z^2 - r^2$ state. The decrease of the difference between the $W_{3z^2-r^2}$ and $W_{x^2-y^2}$ bandwidths from $U = 0$ up to 5 eV in Fig. 5(c), coming from the increase of $W_{3z^2-r^2}$, promotes the DEX interactions mediated by itinerant electrons, Fig. 5(b). Further, the positive (FM) contribution to the exchange interaction changes its sign at about $U = 7$ eV, where a sharp decrease of the $W_{3z^2-r^2}$ value for the FM phase occurs. In addition, due to a redistribution of the electron density between states, $W_{x^2-y^2}$ increases slightly, and so the splitting of these two e_g-sub-bands increases. Thus, Coulomb correlations supress the DEX contributions to the interlayer exchange interaction energy, and we believe that the sharp $3z^2 - r^2$ bandwidth narrowing in the range of $6 < U < 7$ eV is responsible for the FM instability, and hence, is the mechanism that produces the change in magnetic ordering. In addition, this splitting of the e_g states promotes strong anisotropy in the electrical transport, as described above.

4. Conclusion

In summary, we have calculated the electronic structure of double-layered $LaSr_2Mn_2O_7$ using both the LSDA and LSDA + U methods and have investigated the influence of the Coulomb interaction parameter on both the electronic structure and the magnetic ordering. The main factors governing band formation in $LaSr_2Mn_2O_7$ are: (i) the exchange splitting with almost unoccupied minority-spin Mn-3d states; (ii) the ligand field splitting of the t_{2g} and e_g states; and (iii) further splitting of the e_g states with increase of U. We consider (iii) an essential factor in the layered manganites. We have examined FM and A-type AFM ground states of this compound by comparing their total energy differences for a number of U values (from 0 to 10 eV) and found that the experimentally observed magnetic ordering is reproduced within LSDA + U only for $U \geqslant 7$ eV—in contrast with the 3D manganites ($LaMnO_3$) where LSDA gives the true magnetic ground state. It was shown that the correlations reduce significantly the effective hopping parameter for the electrically active e_g electrons along the c-axis, so that taking into account the Coloumb correlation gives the correct 2D-picture in the layered manganite. The strong anisotropy in electrical transport which we obtained is consistent with observations of anisotropic transport—a property which sets this manganite apart from conventional 3D systems.

Acknowledgements

Work at Northwestern University was supported by the US Department of Energy (Grant No. DE-F602-88ER45372).

References

[1] Y. Moritomo, A. Asamitsu, H. Kuwahara, Y. Tokura, Nature (London) 380 (1996) 141.
[2] T. Kimura, Y. Tomioka, H. Kuwahara, A. Asamitsu, M. Tamura, Y. Tokura, Science 274 (1996) 1698.
[3] T.G. Perring, G. Aeppli, Y. Moritomo, Y. Tokura, Phys. Rev. Lett. 78 (1997) 3197.
[4] T. Kimura, Y. Tomioka, A. Asamitsu, Y. Tokura, Phys. Rev. Lett. 81 (1998) 5920.
[5] S. Rosenkranz, R. Osborn, J.K. Mitchell, L. Vasiliu-Doloc, J.W. Lynn, S.K. Sinha, D.N. Argyriou, J. Appl. Phys. 83 (1998) 7348.

[6] M. Kubota, H. Yoshizawa, Y. Moritomo, H. Fujioka, K. Hirota, Y. Endoh, J. Phys. Soc. Japan 68 (1999) 2202.
[7] A. Urushibara, Y. Moritomo, T. Arima, A. Asamitsu, G. Kido, Y. Tokura, Phys. Rev. B 51 (1995) 14 103.
[8] P.D. Battle, D.E. Cox, M.A. Green, J.E. Millburn, L.E. Spring, P.G. Radaelli, M.J. Rosseinsky, J.F. Vente, Chem. Mater. 9 (1997) 1042.
[9] M. Kubota, H. Fujioka, K. Ohoyama, K. Hirota, Y. Moritomo, H. Yoshizawa, Y. Endoh, J. Phys. Chem. Solids 60 (1999) 1161.
[10] Y. Moritomo, Y. Maruyama, T. Akimoto, A. Nakamura, J. Phys. Soc. Japan 67 (1998) 405.
[11] T. Hayashi, N. Miura, M. Tokunaga, T. Kimura, Y. Tokura, J. Phys.: Condens. Matter 10 (1998) 11 525.
[12] D.N. Argyriou, H.N. Bordallo, B.J. Campbell, A.K. Cheetham, D.E. Cox, J.S. Gardner, K. Hanif, A. dos Santos, G.F. Strouse, Phys. Rev. B 61 (2000) 15 269.
[13] T. Chatterji, G.J. McIntyre, W. Caliebe, R. Suryanarayannan, G. Dhalenne, A. Revcolevschi, Phys. Rev. B 61 (2000) 570.
[14] E.O. Wollan, W.C. Koehler, Phys. Rev. 100 (1955) 545.
[15] W.E. Pickett, D.J. Singh, Phys. Rev. B. 53 (1996) 1146.
[16] P.K. Boer, R.A. de Groot, Phys. Rev. B 60 (1999) 10 758.
[17] D.S. Dessau, T. Saitoh, C.-H. Park, Z.-X. Shen, P. Villella, N. Hamada, Y. Moritomo, Y. Tokura, Phys. Rev. Lett. 81 (1998) 192.
[18] O.K. Andersen, Phys. Rev. B 12 (1975) 3060.
[19] U. von Barth, L. Hedin, B. Janak, Phys. Rev. B 12 (1975) 1257.
[20] O. Gunnarsson, O.K. Andersen, O. Jepsen, J. Zaanen, Phys. Rev. B 39 (1989) 1708.
[21] V.I. Anisimov, O. Gunnarsson, Phys. Rev. B 43 (1991) 7570.
[22] V.I. Anisimov, J. Zaanen, O.K. Andersen, Phys. Rev. B 44 (1991) 943.
[23] V.I. Anisimov, F. Aryasetiawan, A.I. Lichtenstein, J. Phys.: Condens. Matter 9 (1997) 767.
[24] S. Satpathy, Z.S. Popovic, F.R. Vukajlovic, Phys. Rev. Lett. 76 (1996) 960.
[25] I. Solovyev, N. Hamada, K. Terakura, Phys. Rev. B 53 (1996) 7158.
[26] X. Huang, O. Mryasov, D. Novikov, A.J. Freeman, Phys. Rev. B 62 (2000) 13 318.
[27] Z. Fang, I.V. Solovyev, K. Terakura, Phys. Rev. Lett. 84 (2000) 3169.
[28] J.Y.T. Wei, N.-C. Yeh, R.P. Vasquez, Phys. Rev. Lett. 79 (1997) 5150.
[29] J.-H. Park, E. Vescovo, H.-J. Kim, C. Kwon, R. Ramesh, T. Venkatesan, Nature (London) 392 (1998) 794.
[30] A.I. Lichtenstein, J. Zaanen, V.I. Anisimov, Phys. Rev. B 52 (1995) R5467.